PERGAMON

Computers and Structures 80 (2002) 515–531

Computers & Structures

www.elsevier.com/locate/compstruc

Post-limit stiffness and ductility of end-plate beam-to-column steel joints

L. Simões da Silva [a,*], Aldina Santiago [b], Paulo Vila Real [c]

[a] Department of Civil Engineering, University of Coimbra, Polo II, Pinhal de Marrocos, 3030 Coimbra, Portugal
[b] Department of Civil Engineering, University of Beira Interior, Edifício II das Engenharias, Calçada do Lameiro, 6200 Covilhã, Portugal
[c] Department of Civil Engineering, University of Aveiro, Campo de Santiago, 3800 Aveiro, Portugal

Received 26 July 2001; accepted 9 January 2002

Abstract

A procedure for the evaluation of ductility in steel joints is presented. Using the component method as background, a non-linear analysis for a number of end-plate beam-to-column joints is performed that is capable of identifying the "yield" sequence of the various components and the failure of the joint. Each component is characterised using a bi-linear approximation for the force–displacement relation. Comparing these results with the corresponding experimental results leads to a proposal of the post-limit stiffness of the various components. A component ductility index is proposed for each component as a means of classification with respect to ductility, using the three ductility classes currently proposed in the literature. A joint ductility index is also proposed, which can be used to verify available rotation against the structure required rotation.

Keywords: Steel joints; Steel structures; Ductility; Component method; Post-limit stiffness

1. Introduction

It is never enough repeating that the behaviour of joints is complex, falling between the traditional assumption of pinned or fully rigid response. A considerable effort was undertaken over the past two decades to give consistent predictions of the behaviour of steel joints. However, until now, most research studies on the behaviour of semi-rigid joints were focused on determining resistance and stiffness characteristics [8,17,19] leading, for example, to the code specifications for the evaluation of strength and stiffness of steel joints that were prepared for Eurocode 3 [2].

The evaluation of joint ductility constitutes an essential characteristic to ensure that sufficient rotation or deformation capacity is available to allow the chosen analysis type (elastic, plastic). Fig. 1 illustrates the moment–rotation response of a very stiff, overstrength joint (rigid in practical terms) that, for a given applied moment M, exhibits a rotation $\theta'_j < \theta_b$, θ_b denoting the corresponding beam rotation. In contrast, for the same applied moment, a semi-rigid joint will reach a rotation $\theta''_j > \theta_b$, thus requiring much higher ductility from the joint. This ductility demand may easily reach 0.03 rad for some joints where a plastic hinge is required, in plastic design conditions.

The prediction of the deformation of beam-to-column or beam-to-beam steel joints requires the consideration of bending moments and axial and shear forces, that are usually present in a steel frame. Concentrating solely on the rotational deformations arising from bending moments of the connected beam, it is necessary to define the various contributions for the total rotation of the joint. In analogy with member rotation, and given that non-linearity in the moment–rotation response of steel connections starts at low values of rotation, ductility ratios are proposed in this paper, aimed at the

* Corresponding author. Tel.: +351-239-797216; fax: +351-239-797217.
E-mail address: luis_silva@gipac.pt (L. Simões da Silva).

0045-7949/02/$ - see front matter
PII: S0045-7949(02)00014-7

Nomenclature

A	cross-section area
A_s	tensile stress area of the bolt
A_c	effective web area in compression zone
A_t	effective web area in tension zone
A_w	effective shear area
A_{wc}	shear area of the column
$B_{t,Rd}$	tensile resistance of bolts
E	Young's modulus
F^y	strength of component
$F_{b,fc,Rd}$	resistance of column flange in bending
$F_{b,p,Rd}$	resistance of end-plate in bending
$F_{c,fb,Rd}$	compression resistance of a beam flange and the adjacent compression zone of a beam web
$F_{c,wc,Rd}$	resistance of an unstiffened column web subject to transverse compression
$F_{t,wb,Rd}$	tensile resistance of the beam web
$F_{t,wc,Rd}$	tensile resistance of the column web
$F_{v,Rd}$	shear resistance of bolts
G	shear modulus of steel
K^e	elastic stiffness of the connection, obtained from the following: k_iE
K^{pl}	post-limit stiffness of the connection
$K_{b,f}$	stiffness of component column flange in bending
$K_{b,p}$	stiffness of component end-plate in bending
$K_{c,wc}$	stiffness of component column web in compression
$K_{t,b}$	stiffness of component bolt in tension
$K_{t,wb}$	stiffness of component beam web in tension
$K_{t,wc}$	stiffness of component column web in tension
K_w	stiffness of component weld
K_{wp}	stiffness of component column web panel in shear
L_b	bolt elongation length, taken as equal to the grip length (total thickness of material and washers), plus half the sum of the height of the bolt head and the height of the nut
M	moment
$M_{c,Rd}$	moment resistance of the beam cross-section, reduced if necessary to allow for shear
$M_{pl,Rd}$	flexural resistance of end-plate or column flange
Q	shear force of the column web
$V_{wc,Rd}$	shear resistance of column web panel
a	effective thickness of the weld
b	flange width
b_{eff}	effective width
$b_{eff,c,wc}$	effective width of the column in compression zone
$b_{eff,t,wb}$	effective width of the beam web in tension zone
$b_{eff,t,wc}$	effective width of the column web in tension zone
d_b	clear depth of the beam
d_c	clear depth of the column
f_u	ultimate tensile strength of the weld
f_{ub}	ultimate tensile strength of the bolts
f_y	yield stress
$f_{y,p}$	yield stress of end-plate
$f_{y,wb}$	yield stress of a beam web
$f_{y,wc}$	yield stress of a column web
h	depth of the column
h_t	distance from the tensile force to the centre of compression
l_{eff}	smallest of the effective lengths (individually or as part of a bolt group)
k_i	stiffness coefficients for basic joint components
m	distance between the bolt centre-line and the face of the weld connecting the beam web to the end-plate; number of faying surfaces or shear planes in a bolted joint, equal to 1.0 for bolts in single shear and 2.0 for bolts in double shear
n	effective distance to the free edge
n_b	number of bolt-rows
r	root radius of the web-flange junction
t_f	flange thickness
t_{fb}	thickness of a beam flange
t_{fc}	thickness of a column flange
t_p	thickness of end-plate
t_w	web thickness
t_{wb}	thickness of a beam web
t_{wc}	thickness of a column web
z	lever arm between the compressive resistance, and tensile resistance
v	Poisson's ratio
β	transformation parameter, see Part 1–8, EC3
β_w	correlation factor
θ	rotation
θ'_j; θ''_j; θ_b	design rotation to rigid joint; semi-rigid joint and beam, respectively
ω	reduction factor to allow for the possible effects of shear in the column web panel
ρ	reduction factor for plate buckling
Δ^y	deformation that correspond to yield stress
Δ^f	deformation that correspond to failure
Δ_i	deformation for basic joint components

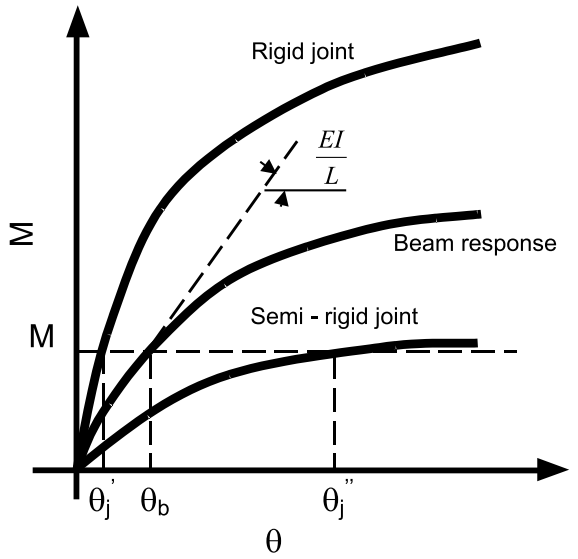

Fig. 1. Comparison of moment–rotation response between beam and various joint types.

objective of ensuring ductility compliance, within the framework of the component method, as explained later in this paper.

2. Joint models

2.1. Component method

Identification of the various components that constitute a joint (bolts, welds, stiffeners) gives a good picture of the complexity of its analysis, which requires proper consideration of a multitude of phenomena, ranging from material non-linearity (plasticity, strain-hardening), non-linear contact and slip, geometrical non-linearity (local instability) to residual stress conditions and complicated geometrical configurations. Although numerical approaches using non-linear finite elements may deal with all these complexities, they require lengthy procedures and are very sensitive to the modelling and analysis options. In practical terms, a predictive approach must thus be based on simpler models that eliminate much of the variability arising from the analysis procedure itself. The so-called component method corresponds precisely to a simplified mechanical model composed of extensional springs and rigid links, whereby the joint is simulated by an appropriate choice of rigid and flexible components. These components represent a specific part of a joint that, dependent on the type of loading, make an identified contribution to one or more of its structural properties [17], as illustrated in Fig. 2a. Typical examples of

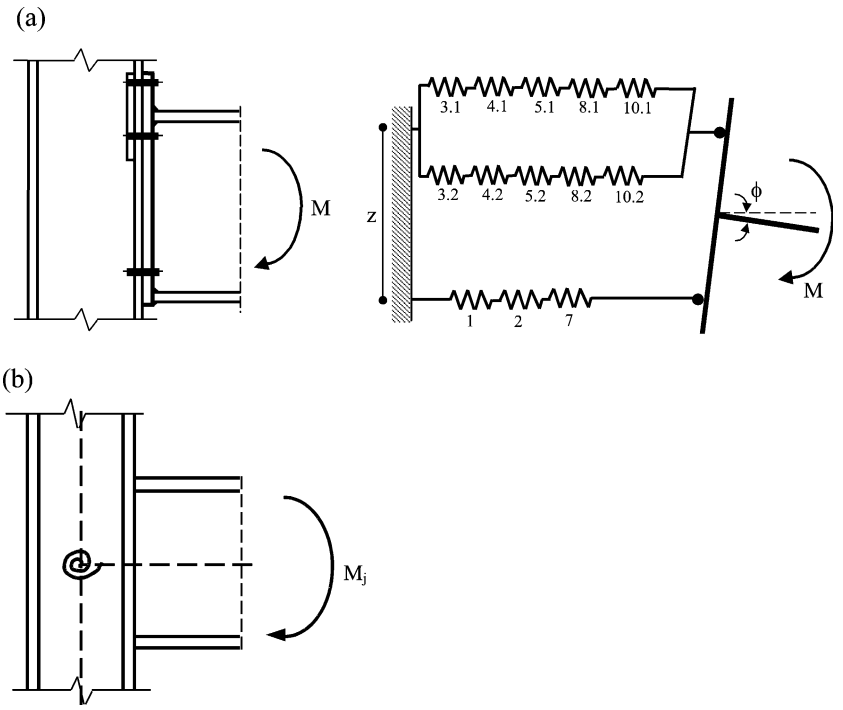

Fig. 2. Component method applied to a typical beam-to-column joint: (a) component model; (b) equivalent rotational spring.

components for bolted steel joints are (i) column web panel in shear, (ii) end-plate in bending, (iii) column flange in bending, (iv) beam web in tension, (v) column web in compression, (vi) column web in tension, (vii) beam flange and web in compression, (viii) bolts in tension and (ix) welds. In general, each of these components is characterised by a non-linear force–deformation curve, although simpler idealisations are possible.

Several alternative spring and rigid link models have been proposed [6], which share the same basic components. In the following, the simplified component model of the revised Annex J of EC3 (1998) will be selected, that, for simplicity, combines the bending behaviour of the joint with the shear behaviour of the column panel to yield an equivalent rotational spring, as shown in Fig. 2b.

Application of the component method to steel joints requires the following steps:

(i) selection of the relevant (active) components from a global list of components (13 different components currently codified, for example, in Annex J of EC3);
(ii) evaluation of the force–deformation response of each component;
(iii) assembly of the active components for the evaluation of the moment–rotation response of the joint, using a representative mechanical model (Fig. 2a).

Its application may correspond to different levels of refinement, simplified characterisation of the components being possible whenever only the resistance or the initial stiffness of the joint is required.

2.2. Component characterisation

Describing the mechanical behaviour of the various components of a joint allows the analysis of a large number of different joint configurations with a relatively small number of repeating components. A key aspect to the component method thus relates to the characterisation of the force–deformation curves for each individual extensional spring. For the evaluation of the initial stiffness of a joint, only the linear stiffness of each component is required, whereas the evaluation of ductility requires the knowledge of the non-linear force–deformation response of each component.

Concentrating on the components relevant for steel beam-to-column joints, a brief review of their behaviour is presented below. With reference to Fig. 3a, it is noted that analytical expressions are only presented for strength and initial stiffness because of lack of data for the post-limit response, here presented only in a qualitative way, according to research results from various authors. Of particular relevance to a ductility evaluation is the deformation capacity of each component. Here, in

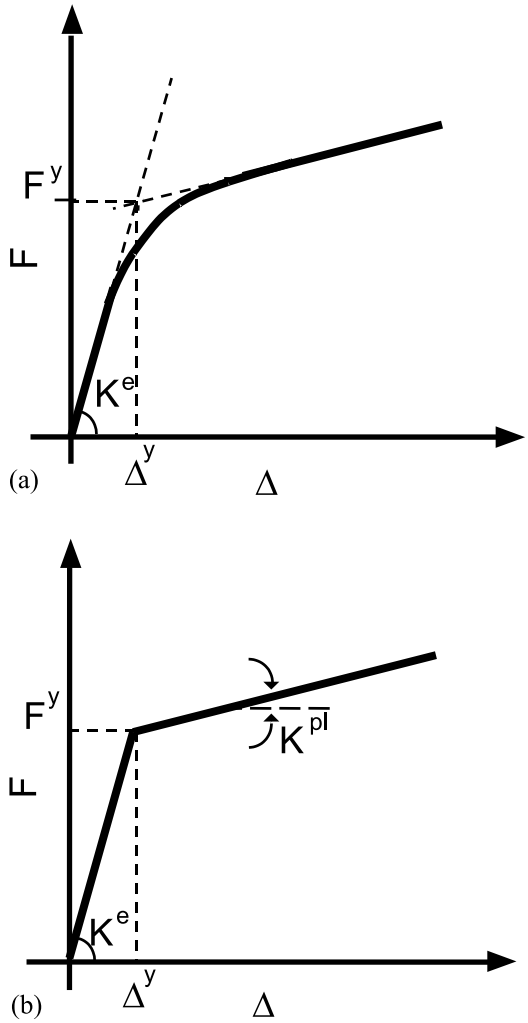

Fig. 3. Components with high ductility: (a) actual behaviour; and (b) bi-linear approximation.

direct analogy with the classification of cross-sections, three classes are proposed [10], described below.

2.2.1. Components with high ductility

According to Kuhlmann et al. [10], these components present a force–deformation curve that changes from an initial linear elastic mode into a second carrying mode which allows increasing deformation with increasing force. The deformation capacity of the component is nearly unlimited, not imposing any bounds on the overall rotation ability of the joint, and is typically illustrated in Fig. 3a or, as a bi-linear approximation, in Fig. 3b, where K^{e}, K^{pl}, F^{y} and Δ^{y} denote, respectively, the initial elastic stiffness, the post-limit stiffness, the strength and the yield displacement of the component. It is noted that Δ^{f}, the limit displacement of the compo-

nent, is very high, so that, in practical terms, Δ^f/Δ^y may be taken as infinity. Some components falling into this classification are described below:

2.2.1.1. Column web panel in shear. This component has been studied by Jaspart [8], typical experimental results being reproduced in Fig. 4, that clearly show the stable post-limit response.

The resistance of the panel zone in shear is given by

$$V_{wp,Rd} = \frac{f_{y,wc} A_{wc}}{\sqrt{3}} \tag{1}$$

where $f_{y,wc}$ is the yield stress of the column web and A_{wc} is the shear area of the column. In case of welded sections, the shear area of the column coincides with the area of the web, whereas in the case of rolled sections it is given by

$$A_{wc} = A_c - 2b_c t_{fc} + (t_{wc} + 2r_c)t_{fc} \tag{2}$$

where A_c is the total area of the column, b_c, t_{fc} and t_{wc} are, respectively, the flange width, the flange thickness and the web thickness of the column and r_c is the root-radius of the web-flange junction. Eq. (1) neglects the column axial load; otherwise, using the Von Mises yield criterion it would be possible to evaluate a reduced value of resistance that takes the column axial load into consideration. Jaspart [8] suggested a reduction coefficient of 0.9 that approximately takes care of this problem, an approach currently adopted in Annex J of EC3, yielding

$$V_{wc,Rd} = \frac{0.9 f_{y,wc} A_{wc}}{\sqrt{3}} \tag{3}$$

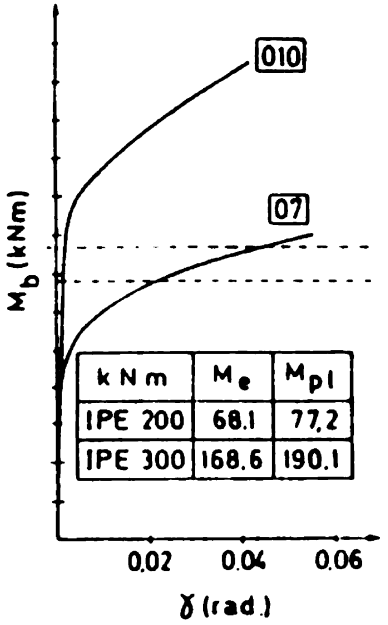

Fig. 4. Experimental results taken from Jaspart [8].

According to Janss and Jaspart [7], Jaspart [8] and Shi et al. [16], the contribution of the shear deformation of the column web panel to the overall initial rotation of the joint is given by

$$\Phi_s = \frac{Q}{GA_{wc}} \tag{4}$$

where Q denotes the shear force on the column web, taken as $2\sum F_i$ (F_i denoting the force in each bolt row and i the bolt row), and A_{wc} already defined above. The corresponding axial stiffness becomes

$$K_{wp} = \frac{GA_{wc}}{z} = \frac{0.38EA_{wc}}{z} \tag{5}$$

where z denotes the lever arm between the compressive and the tensile areas. From Eq. (4) it can be observed that the stiffness of this component depends on the applied shear force on the column web. Given that, in general, internal forces transmitted by the lower and upper column and (for internal nodes with unbalanced moments) left beam may also be present, the applied shear force must also be modified by a factor β to deal with this effect, Eq. (5) becoming

$$K_{wp} = \frac{0.38EA_{wc}}{\beta z} \tag{6}$$

For a stiffened web panel the shear deformation may be neglected ($K_{s,wp} = \infty$). Finally, it should be noted that for slender webs, instability becomes the governing factor, currently not covered in code specifications.

2.2.1.2. End-plate in bending. The deformation of this component is usually evaluated using a simple substitute model, the T-stub [18,19], assumed to represent the behaviour of the tension zone of the joint and illustrated in Fig. 5a. In terms of resistance, the T-stub exhibits three

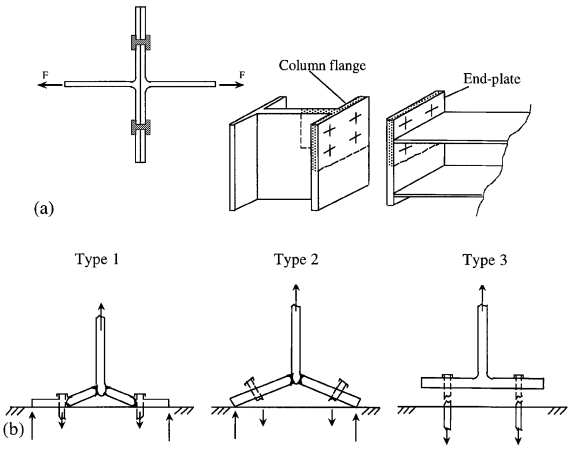

Fig. 5. Equivalent T-stub assembly.

alternative failure modes, typically shown in Fig. 5b, described next:

(i) Type 1—end-plate yielding without bolt failure.
(ii) Type 2—simultaneous yielding of end-plate with bolt failure.
(iii) Type 3—bolt failure without end-plate yielding.

Eq. (7) describes the corresponding axial strength,

$$F_{t,Rd} = \begin{cases} \dfrac{4M_{pl,Rd}}{m} & \text{Type 1} \\ \dfrac{2M_{pl,Rd} + n\sum B_{t,Rd}}{m+n} & \text{Type 2} \\ \sum B_{t,Rd} & \text{Type 3} \end{cases} \quad (7)$$

where m denotes the distance between the bolt centre-line and the face of the weld connecting the beam web to the end-plate, n is the effective distance to the free edge, $B_{t,Rd}$ corresponds to the resistance of the bolts in tension and $M_{pl,Rd}$ is the flexural resistance of the end-plate, given by

$$M_{pl,Rd} = \frac{l_{eff} t_p^2 f_{y,p}}{4} \quad (8)$$

where l_{eff} is the effective width of the end-plate in bending, and t_p and $f_{y,p}$ are the thickness and yield stress of the end-plate, respectively.

Analytical expressions for the initial stiffness of the T-Stub (end-plate in bending) can be derived from classical beam theory [16,18], once an effective width has been properly evaluated, giving

$$K_{b,p} = \frac{0.85 E l_{eff} t_p^3}{m^3} \quad (9)$$

typical force–deformation results obtained from experimental work being reproduced in Fig. 6 [5], showing a stable (positive) post-limit stiffness.

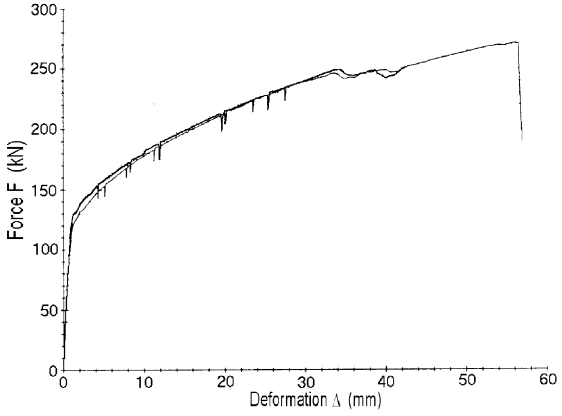

Fig. 6. Force versus deformation for T-Stub assembly taken from Gebbeken et al. [5].

2.2.1.3. Column flange in bending. Except for the restraint provided by additional stiffening of the column, this component behaves similarly to the end-plate in bending, the T-Stub approach being equally valid. The same degree of ductility and post-limit stiffness is thus to be expected, the relevant equations for strength and stiffness being reproduced below.

$$F_{t,Rd} = \begin{cases} \dfrac{4M_{pl,Rd}}{m} & \text{Type 1} \\ \dfrac{2M_{pl,Rd} + n\sum B_{t,Rd}}{m+n} & \text{Type 2} \\ \sum B_{t,Rd} & \text{Type 3} \end{cases} \quad (10)$$

$$K_{b,f} = \frac{0.85 E l_{eff} t_{fc}^3}{m^3} \quad (11)$$

the various quantities having the same meaning as for the end-plate in bending, just replacing the end-plate for the column flange.

2.2.1.4. Beam web in tension. For bolted end-plate joints, the tension resistance of the beam web is given by

$$F_{t,wb,Rd} = b_{eff,t,wb} t_{wb} f_{y,wb} \quad (12)$$

where the effective width $b_{eff,t,wb}$ should be taken as equal to the effective length of the equivalent T-Stub representing the end-plate in bending and t_{wb} and $f_{y,wb}$ denote, respectively, the thickness of the beam web and the corresponding yield stress. The initial stiffness for this component may be taken as infinity ($K_{t,wb} = \infty$).

2.2.2. Components with limited ductility

These components are characterised by a force–deformation curve exhibiting a limit point and a subsequent softening response, as shown in Fig. 7a or, as a bi-linear approximation, in Fig. 7b. In this ductility class, it is required to define the collapse displacement of the component, Δ^f.

2.2.2.1. Column web in compression. This component has been studied by Kuhlmann [9], who concluded that it exhibited limited ductile behaviour with a softening branch after reaching its maximum load carrying capacity, as reproduced in Fig. 8.

The resistance of this component may be subdivided into two different criteria, crushing and buckling resistance. The crushing resistance must take into account the interaction between local stresses that arise from the shear stresses in the panel zone, the vertical normal stresses due to axial load and bending moment in the column and the horizontal normal stresses transmitted by the beam flanges. Using the Von Mises yield criterion [4], the crushing resistance is given by

$$F_{c,wc,Rd} = b_{eff,c,wc} t_{wc} f_{y,wc} \omega k_{c,wc} \quad (13)$$

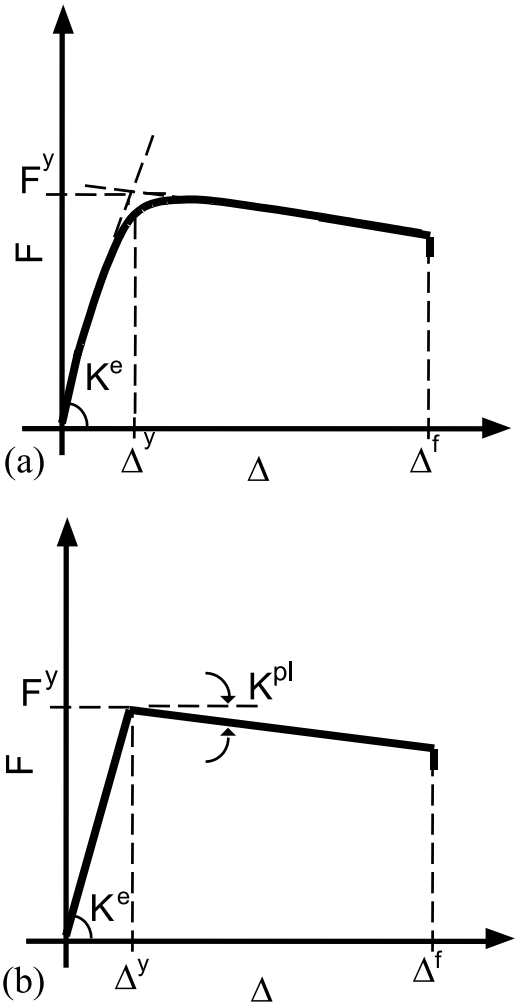

Fig. 7. Components with limited ductility: (a) actual behaviour; and (b) bi-linear approximation.

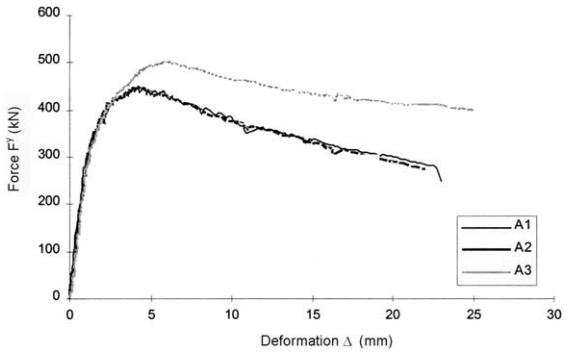

Fig. 8. Force–deformation response of column web in compression [9].

where $b_{\mathrm{eff,c,wc}}$ is the effective width of the column web in compression, given by, for bolted end-plate joints,

$$b_{\mathrm{eff,c,wc}} = t_{\mathrm{fb}} + 2\sqrt{2}a + 5(t_{\mathrm{fc}} + s) + s_{\mathrm{p}} \tag{14}$$

a denoting the effective thickness of the weld, $s = r$ for rolled column sections and s_{p} denoting the length obtained by dispersion at 45° through the end-plate; $k_{\mathrm{c,wc}}$ accounts for the influence of vertical normal stress, σ_{v},

$$k_{\mathrm{c,wc}} = 1.25 - 0.5\frac{\sigma_{\mathrm{v}}}{f_{\mathrm{y,wc}}} \leqslant 1 \quad (\sigma_{\mathrm{v}} > 0.5 f_{\mathrm{y,wc}}) \tag{15}$$

and ω accounts for the shear interaction, given by [8]

$$\omega = \begin{cases} 1 & 0.0 \leqslant \beta \leqslant 0.5 \\ \omega_1 + 2(1-\beta)(1-\omega_1) & 0.5 \leqslant \beta \leqslant 1.0 \\ \omega_1 + (\beta - 1)(\omega_2 - \omega_1) & 1.0 \leqslant \beta \leqslant 2.0 \end{cases} \tag{16}$$

with

$$\omega_1 = \frac{1}{\sqrt{1 + 1.3(b_{\mathrm{eff,c,wc}} t_{\mathrm{wc}}/A_{\mathrm{vc}})^2}} \tag{17a}$$

$$\omega_2 = \frac{1}{\sqrt{1 + 5.2(b_{\mathrm{eff,c,wc}} t_{\mathrm{wc}}/A_{\mathrm{vc}})^2}} \tag{17b}$$

The buckling resistance is taken approximately using the Winter formula as

$$F_{\mathrm{c,wc,Rd}} \leqslant \rho b_{\mathrm{eff,c,wc}} t_{\mathrm{wc}} f_{\mathrm{y,wc}} \omega k_{\mathrm{c,wc}} \tag{18}$$

where ρ denotes the reduction factor for plate buckling, given by

$$\rho = \begin{cases} 1 & \bar{\lambda} < 0.673 \\ \frac{(\bar{\lambda} - 0.22)}{\bar{\lambda}^2} & \bar{\lambda} > 0.673 \end{cases} \tag{19}$$

and $\bar{\lambda}$ denotes the normalised plate slenderness,

$$\bar{\lambda} = \sqrt{\frac{b_{\mathrm{eff,c,wc}} t_{\mathrm{wc}} f_{\mathrm{y,wc}}}{F_{\mathrm{cr}}}} = 0.932\sqrt{\frac{b_{\mathrm{eff,c,wc}} d \times f_{\mathrm{y,wc}}}{E t_{\mathrm{wc}}^2}} \tag{20}$$

The initial deformation of this component, Φ_{c}, may be determined from [16]

$$\Phi_{\mathrm{c}} = \frac{N}{EA_{\mathrm{c}}}\frac{d}{h_{\mathrm{c}}} \tag{21}$$

where N is the resultant compressive force, taken as $2\sum F_i$ (F_i denote the force in each bolt row and i the bolt row), A_{c} is the effective web area in compression zone, $A_{\mathrm{c}} = t_{\mathrm{wc}} b_{\mathrm{eff,c}}$, d the depth between column fillets, and h_{c} the beam depth minus beam flange thickness, so that the initial (axial) stiffness becomes

$$K_{\mathrm{c,wc}} = EA_{\mathrm{c}}\frac{1}{d} = E\frac{0.7 b_{\mathrm{eff,c,wc}} t_{\mathrm{wc}}}{d} \tag{22}$$

where it is noted that for the stiffness calculation a reduction of the effective width used for the strength calculation is adopted ($0.7b_{\text{eff,c,wc}}$).

2.2.2.2. Column web in tension. Excluding instability phenomena, the resistance of this component is similar to the column web in compression. Consequently,

$$F_{\text{t,wc,Rd}} = b_{\text{eff,t,wc}} \times t_{\text{wc}} \times f_{\text{y,wc}} \times \omega \times k_{\text{t,wc}} \tag{23}$$

where the various quantities take the same meaning as before by replacing c for t. It is noted that Annex J of EC3 disregards the influence of vertical stresses arising from the column.

In analogy with the previous case, the initial deformation of this component, Φ_{w}, may be determined from [16]

$$\Phi_{\text{w}} = \frac{T}{EA_{\text{t}}}\frac{d}{h_{\text{t}}} \tag{24}$$

where T is the resultant tensile force, taken as $2\sum F_i$ (F_i denoting the force in each bolt row and i the bolt row), A_{t} is the effective web area in the tensile zone, $A_{\text{t}} = t_{\text{wc}} b_{\text{eff,t,wc}}$, d the depth between column fillets, and h_{t} the distance from the tensile force to the center of compression, so that the axial stiffness becomes

$$K_{\text{t,wc}} = EA_{\text{t}}\frac{1}{d} = E\frac{0.7b_{\text{eff,t,wc}}w_{\text{c}}}{d} \tag{25}$$

2.2.2.3. Beam flange and beam web in compression. The beam flange and web in compression adjacent to the beam-connection system provides a limitation to the resistance of the joint, so that it is required to assess its maximum resistance, given by

$$F_{\text{c,fb,Rd}} = \frac{M_{\text{c,Rd}}}{z} \tag{26}$$

while its initial stiffness is taken as infinity.

2.2.3. Components with brittle failure

These components behave linearly until collapse, with very little deformation before failure, as shown in Fig. 9a or, as a linear approximation, in Fig. 9b, so that $\Delta^{\text{f}} = \Delta^{\text{y}}$.

2.2.3.1. Bolts in tension. Bolts exhibit a linear force–deformation response up to failure, as shown in Fig. 10, taken from a tensile test on a single bolt. The resistance and initial stiffness of each bolt are given by

$$F_{\text{t,Rd}} = 0.9f_{\text{ub}}A_{\text{s}} \tag{27}$$

$$K_{\text{t,b}} = \frac{1.6EA_{\text{s}}}{L_{\text{b}}} \tag{28}$$

where A_{s} is the tensile area of the bolt, f_{ub} the ultimate tensile strength of the bolts and L_{b} is the sum of the

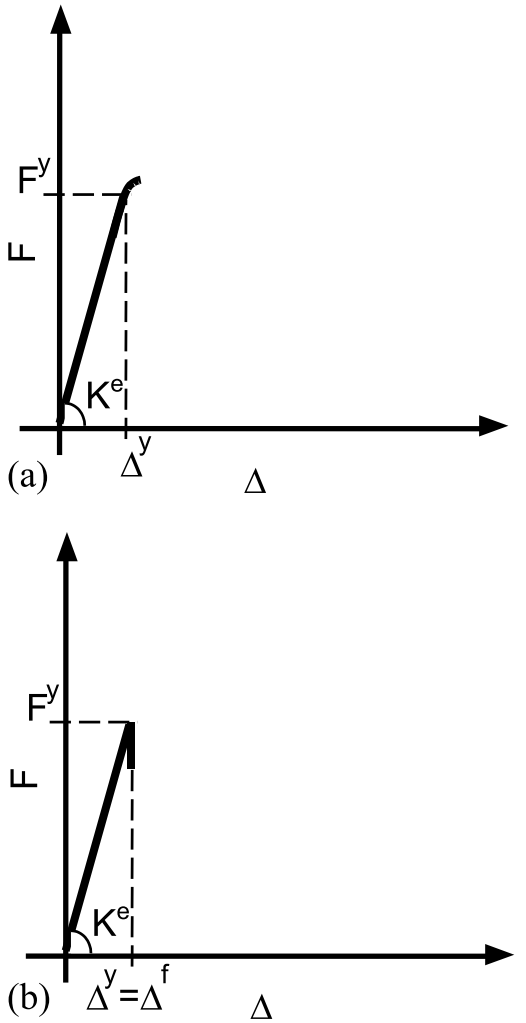

Fig. 9. Components with brittle failure: (a) actual behaviour; and (b) linear approximation.

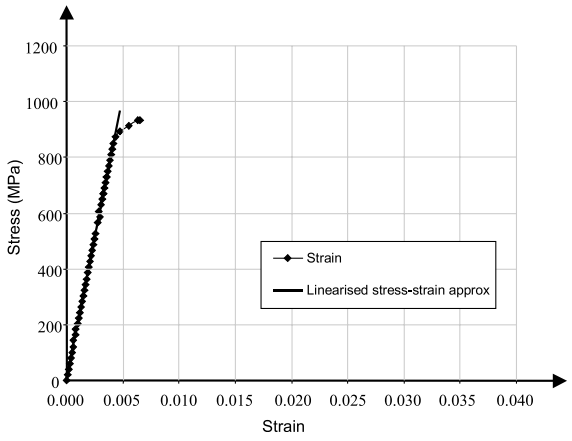

Fig. 10. Experimental results for bolt in tension.

thickness of the connected plates, the thickness of the washers and the half thickness of the nut and the bolt head.

2.2.3.2. Welds. Welds are virtually undeformable ($K_w = \infty$), a rigid-plastic model being adequate, resistance being given by

$$F_{w,Rd} = a\frac{f_u/\sqrt{3}}{\beta_w} \tag{29}$$

where a is the effective thickness of the weld, f_u the ultimate tensile strength of the weld and β_w is a correlation factor.

3. Joint ductility

The assessment of the ductility of a steel joint requires a non-linear procedure, which takes into account the non-linear force–deformation response of each component. Here a bi-linear force–deformation response with a cut-off is assumed which highlights, for each component, the transition between initial elastic stiffness and residual stiffness while maintaining sufficient accuracy. Additionally, direct comparison with ideal linear elastic components is straightforward using, for example, the values for component stiffness that were presented above.

4. Post-limit stiffness of bolted end-plate beam-to-column joints

4.1. Introduction

In order to evaluate realistic values of the post-limit stiffness of the various relevant components, a set of four extended end-plate beam-to-column joints tested by Humer at the University of Innsbruck (1987) were selected from the database of steel joints SERICON II [1].

Table 1
Mechanical properties of Humer tests

Elements	Yield strength (MPa)	Failure strength (MPa)
Humer 109.005		
Column web	306.6	445.0
Column flange	275.9	400.5
Beam web	315.6	398.0
Beam flange	284.6	413.0
End-plate	323.0	360.0
Backing plate	333.0	
Bolts[a]	900.0	1000.0
Humer 109.006		
Column web	309.4	449.0
Column flange	247.6	398.5
Beam web	294.2	427.0
Beam flange	288.0	418.0
End-plate	325.0	360.0
Backing plate	336.0	
Bolts[a]	900.0	1000.0
Humer 109.003		
Column web	341.1	499.0
Column flange	300.4	468.0
Beam web	343.8	458.0
Beam flange	322.5	413.0
End-plate	273.0	360.0
Backing plate	368.0	
Bolts[a]	900.0	1000.0
Humer 109.004		
Column web	359.0	521.0
Column flange	305.9	444.0
Beam web	315.6	458.0
Beam flange	284.6	413.0
End-plate	323.0	360.0
Backing plate	298.0	
Bolts[a]	900.0	1000.0

$E = 210$ GPa.
[a] Nominal values.

For all specimens, the (measured) material properties and geometries are reproduced in Tables 1 and 2, the

Table 2
Geometric properties of Humer tests

	Test			
	109.005	109.006	109.003	109.004
Beam	IPE450R: $h = 454$; $b = 192$; $t_f = 14$; $t_w = 10.4$; $r = 21$	IPE600R: $h = 597$; $b = 220$; $t_f = 18.6$; $t_w = 12.1$; $r = 24$	IPE300R: $h = 300$; $b = 151$; $t_f = 11.2$; $t_w = 7$; $r = 15$	IPE450R: $h = 454$; $b = 192$; $t_f = 14.6$; $t_w = 10.4$; $r = 21$
Column	HEB240R: $h = 242$; $b = 240$; $t_f = 16.4$; $t_w = 10.4$; $r = 21$	HEB240R: $h = 240$; $b = 240$; $t_f = 17$; $t_w = 10.4$; $r = 21$	HEB180R: $h = 179$; $b = 180$; $t_f = 14.1$; $t_w = 9.2$; $r = 15$	HEB180R: $h = 180$; $b = 180$; $t_f = 14$; $t_w = 9.4$; $r = 15$
End-plate	$553 \times 239 \times 41$	$693 \times 243 \times 40$	$383 \times 181 \times 30$	$553 \times 239 \times 41$
Backing-plate	$2 \times 185 \times 100 \times 12$	$2 \times 200 \times 95 \times 12$	$2 \times 150 \times 70 \times 10.8$	$2 \times 185 \times 100 \times 10.4$
Bolts	3 bolt rows × M24	3 bolt rows × M24	3 bolt rows × M20	3 bolt rows × M24

Units: mm.

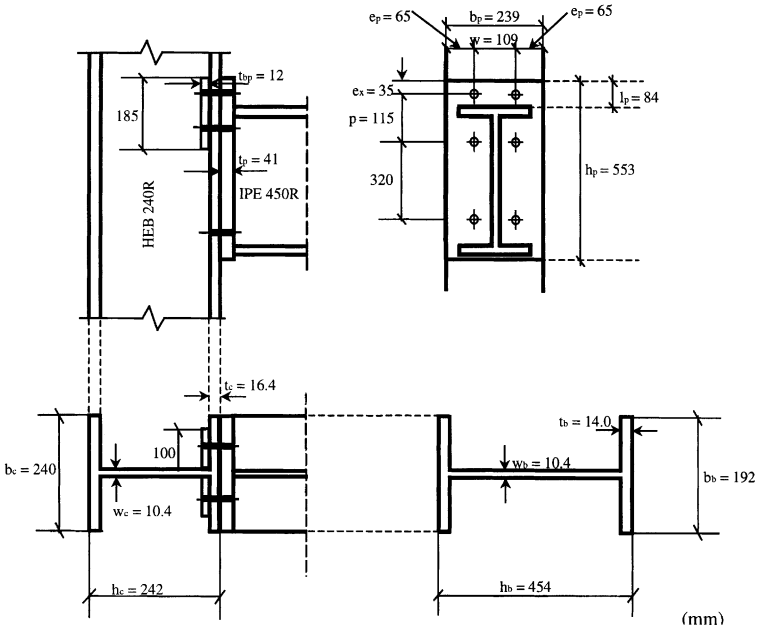

Fig. 11. Joint geometry for Humer 109.005.

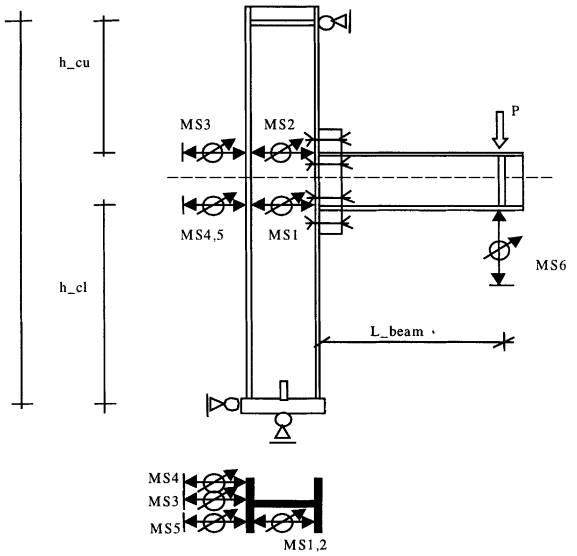

Fig. 12. Localisation of displacement transducers.

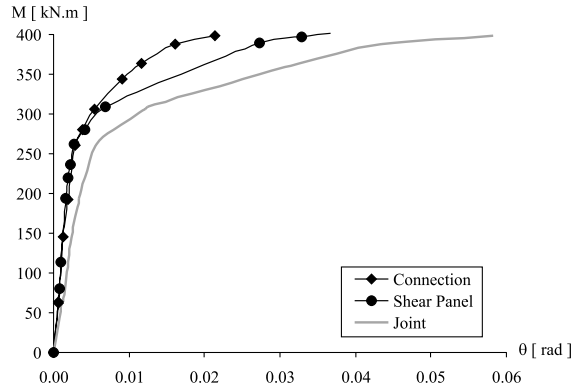

Fig. 13. Experimental results for test Humer 109.005.

layout of the joint, instrumentation and corresponding experimental results for test 109.005 being illustrated in Figs. 11–13.

For each specimen, a prediction of the moment–rotation response was attempted using the component model of Fig. 2a. This component model was analysed either by applying the analytical methodology presented in [14] or by performing a non-linear finite element analysis using the bi-linear characteristics of the components.

The adopted procedure for establishing the post-limit stiffness of the various components involves the following steps:

(a) for each specimen, assumption of trial values of the post-limit stiffness, obtained as a best fit to the experimental moment–total rotation curves;

(b) for each specimen, and where available, best fit calibration of component sub-models with experimental curves for moment versus panel rotation and moment versus connection rotation;
(c) statistical evaluation (mean and standard deviation) of the normalised post-limit stiffness values obtained above (ratio of initial stiffness versus post-limit stiffness) for steps (a) and (b);
(d) for each specimen, evaluation of moment–rotation curves for the average values established above.

5. Numerical models

The numerical model adopted in the analysis for the chosen joint configurations are illustrated in Fig. 14. The rigid links are modelled using beam elements with elastic material properties and very high cross-sectional properties, while the springs are modelled as non-linear joint elements, reproducing the bi-linear characteristics earlier described. An incremental non-linear analysis for an applied bending moment is performed using the non-linear finite element code [12].

According to the procedure defined above, distinct numerical models were defined for step (a) (Fig. 15a: moment versus total joint rotation) and step (b) (Fig. 15b (1): moment versus panel rotation and 15b (2): moment versus connection rotation).

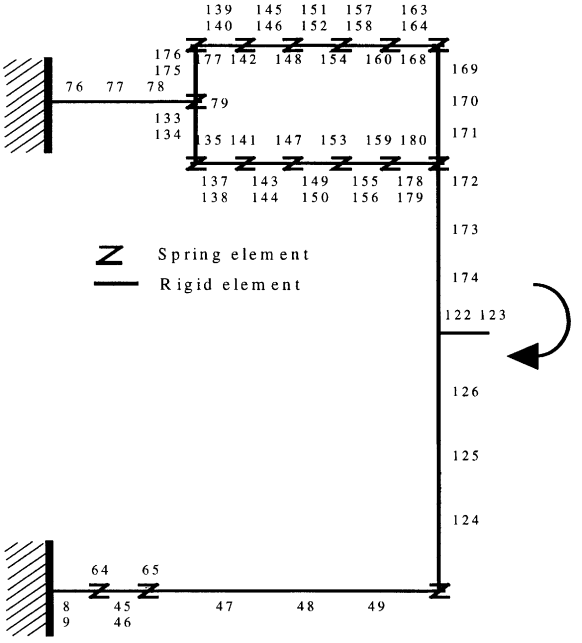

Fig. 14. Finite element model: Humer 109.005.

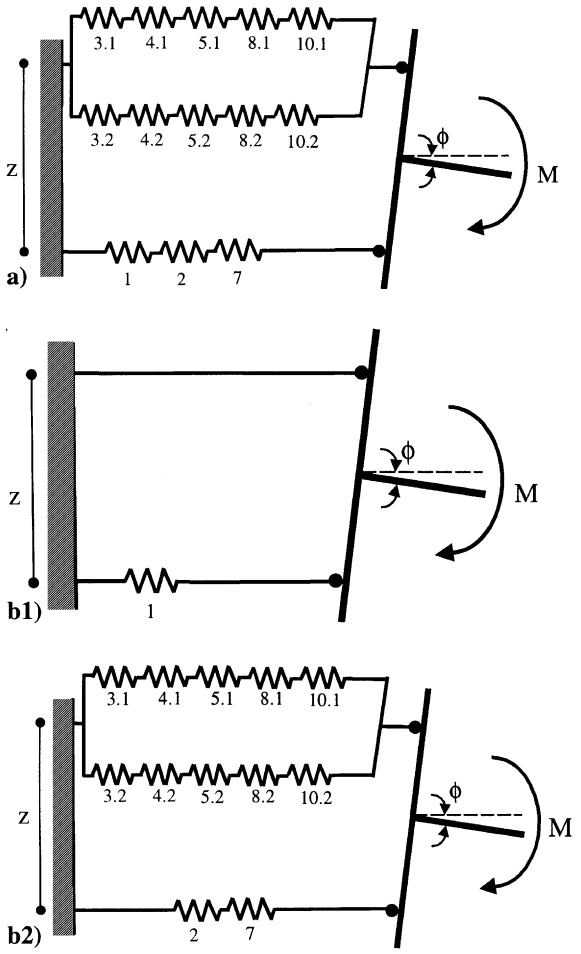

Fig. 15. Component method model: (a) joint model; and (b) (1) shear panel model, (2) connection model.

6. Results and discussion

Starting, for exemplification, with test 109.005, Table 3 reproduces the strength and initial stiffness values for all relevant components. Application of step (a) of the procedure described above leads to the results of Fig. 16, that compares the experimental results with the numerical/analytical results, showing excellent agreement between both curves. For the calculated moment–rotation curve, the yielding rotations of the critical components are also identified. Similarly, application of step (b) yields the results of Fig. 17a and b, that compare the experimental and numerical curves for moment versus panel rotation and moment versus connection rotation, respectively.

Repeating steps (a) and (b) for the remaining joint configurations and defining the normalised post-limit

Table 3
Component characterisation for Humer 109.005

Component	Designation	F^y (kN)	k (mm)	K^e (kN/m)	Δ^y (mm)
Column web in shear	1	543.83	2.91	611100	0.88992
Column web in compression	2	602.31	11.71	2459100	0.24493
Column web in tension	3.1	386.24	7.12	1495200	0.25832
	3.2	386.24	7.12	1495200	0.25832
Column flange in bending	4.1	435.93	17.85	3748500	0.11629
	4.2	435.93	17.85	3748500	0.11629
End-plate in bending	5.1	635.40	114.60	24066000	0.02640
	5.2	635.40	116.87	24542700	0.02589
Beam web in tension	7	877.10	∞	∞	
Beam flange in compression	8.1	941.21	∞	∞	
	8.2	941.21	∞	∞	
Bolts in tension	10.1	635.40	6.25	1312500	0.48411
	10.2	635.40	6.25	1312500	0.48411

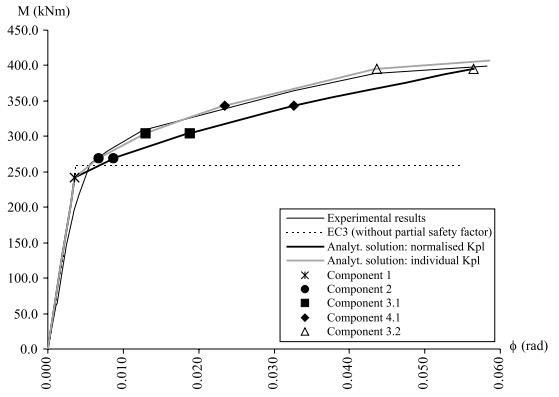

Fig. 16. Moment–rotation curve Humer 109.005 joint.

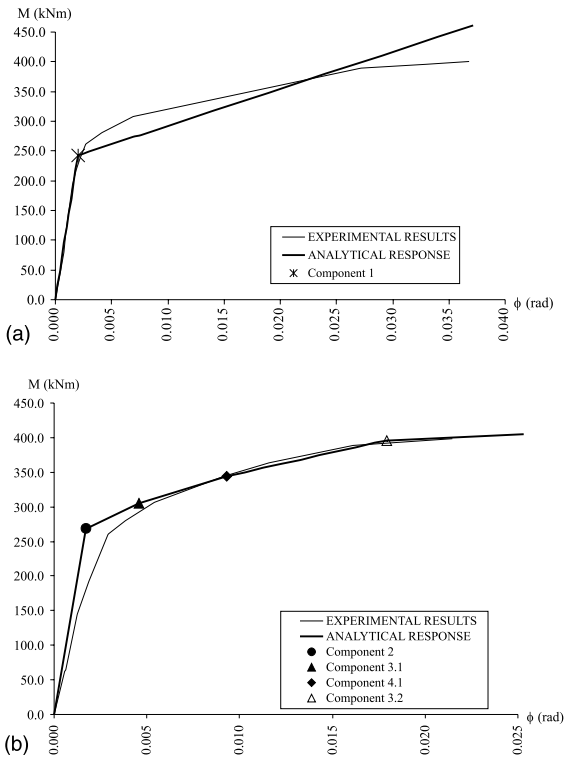

Fig. 17. Moment–rotation curve Humer 109.005: (a) shear panel rotation; and (b) connection rotation.

stiffness as the ratio, expressed as a percentage, between the post-limit stiffness and the corresponding initial stiffness,

$$\overline{K}_i = \frac{K_i^{\mathrm{pl}}}{K_i^{\mathrm{e}}} \times 100 \tag{30}$$

leads to the results of Table 4, that illustrates the calibrated values for the critical components, together with the statistical evaluation (mean and standard deviation) of the normalised post-limit stiffness for each component (step (c)).

Examination of the normalised post-limit stiffness values of Table 4 led to the choice of average values for the various components shown in Table 5. Assuming these mean values for all specimens, and reanalysing all cases using these properties (step (d)) yields the results of Figs. 16,18–20, where the experimental results are plotted superimposed with the numerical results earlier obtained by individual calibration of the post-limit stiffness values ("exact" solution, step (a)) and the corresponding results obtained using the average values of post-limit stiffness.

In order to assess the error of this approach, an adimensional error measure is proposed, given by Eq. (31),

$$\varepsilon = \sqrt{\sum_{i=1}^{n} \varepsilon_i} + \sqrt{\varepsilon_f} \tag{31}$$

Table 4
Calibrated values of post-limit stiffness

		Elastic Stiffness (kN/m)	Moment–total joint rotation		Moment–shear panel/connection rotation	
			Post-limit stiffness (kN/m)	$\overline{K}_i$	Post-limit stiffness (kN/m)	$\overline{K}_i$
Component 1	Humer 109.005	611100	48000	7.86%	33000	5.40%
	Humer 109.006	468300	20000	4.27%	23000	4.91%
	Humer 109.003	573300	27138	4.73%	24000	4.17%
	Humer 109.004	388500	16535	4.26%	15000	3.86%
	Mean			5.28%		4.59%
	Standard deviation			0.016		0.007
Component 2	Humer 109.005	2459100	95000	3.86%	70000	3.05%
	Humer 109.006	2553600	22000	0.86%	34048	1.33%
	Humer 109.003	2362500	92269	3.91%	90865	3.85%
	Humer 109.004	2545200	23622	0.93%	29944	1.17%
	Mean			2.39%		2.35%
	Standard deviation			0.017		0.013
Component 3.1	Humer 109.005	1495200	16988	1.14%	41073	2.75%
	Humer 109.006	1635900	3043	0.19%	42328	2.58%
	Mean			0.66%		2.67%
	Standard deviation			0.007		0.001
Component 4.1	Humer 109.005	3748500	88184	2.35%	52275	1.40%
	Humer 109.006	2499000	14366	0.58%	50023	2.00%
	Humer 109.003	2706900	141912	5.24%	331128	12.23%
	Humer 109.004	1409100	4464	0.32%	7603	0.54%
	Mean (without Humer 109.003)			1.08%		1.31%
	Standard deviation			0.023		0.055
Component 3.2	Humer 109.005	1495200	1048	0.07%	1442	0.10%
	Mean			0.07%		0.1%

Table 5
Adopted normalised post-limit stiffness values for the various components

Component	$\overline{K}_i$ (%)
1	4.59
2	2.35
3.1	1.67
3.2	0.10
4.1	1.31
10.1	7.19
10.2	0.45

where

$$\varepsilon_i = \left(\frac{M_i^{\text{ind}} - M_i^{\text{av}}}{M_i^{\text{ind}}}\right)^2 + \left(\frac{\phi_i^{\text{ind}} - \phi_i^{\text{av}}}{\phi_i^{\text{ind}}}\right)^2 \tag{32}$$

M_i^j denoting the moment at yield of component i, superscript j ($=\text{ind}, \text{av}$) denoting individual calibration (step (a)) or use of average values (step (d)). Similarly, ϕ_i denotes the corresponding joint rotation at yield of component i. The second term in Eq. (31) estimates (where applicable) the error at failure of the joint, given by

$$\varepsilon_{\text{f}} = \left(\frac{M_{\text{f}}^{\text{ind}} - M_{\text{f}}^{\text{av}}}{M_{\text{f}}^{\text{ind}}}\right)^2 + \left(\frac{\phi_{\text{f}}^{i} - \phi_{\text{f}}^{\text{av}}}{\phi_{\text{f}}^{\text{ind}}}\right)^2 \tag{33}$$

M_{f} and ϕ_{f} having the same meaning as before, subscript f denoting failure of the joint. Table 6 illustrates the error for each test.

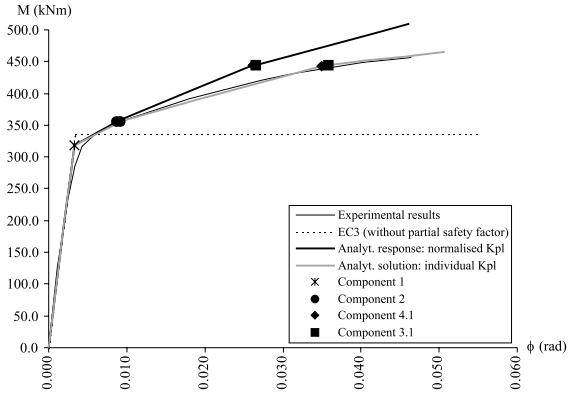

Fig. 18. Humer 109.006: moment–rotation curve, experimental results and analytical response.

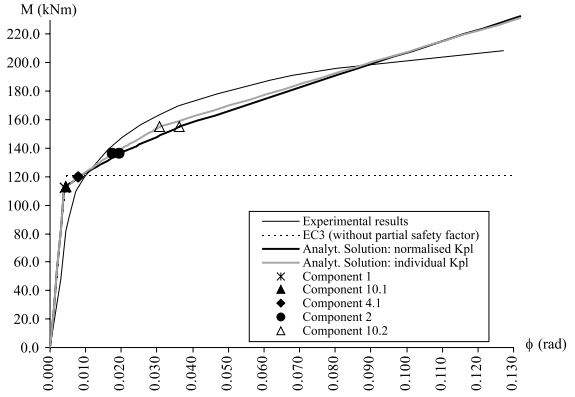

Fig. 19. Humer 109.003: moment–rotation curve, experimental results and analytical response.

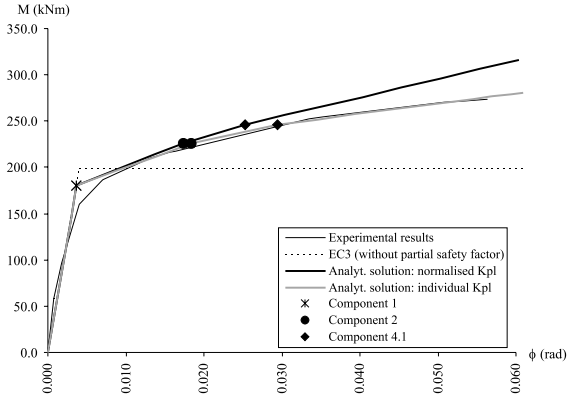

Fig. 20. Humer 109.004: moment–rotation curve, experimental results and analytical response.

Table 6
Error evaluation for teach test result

Humer	Error (%)
109.005	7.871
109.006	3.863
109.003	1.555
109.004	1.857

7. Component ductility index

7.1. Definition

The evaluation of the ductility of steel joints in the context of the component method requires, as mentioned above, the characterisation of the ductility of each component, i.e., the identification of the failure displacement, Δ^{f}, of each component. Here, assuming the bi-linear idealisation of component behaviour of Fig. 7b, a ductility index φ_i is proposed for each component i, defined as,

$$\varphi_i = \frac{\Delta_i^{\mathrm{f}}}{\Delta_i^{\mathrm{y}}} \tag{34}$$

The component ductility index φ_i allow a direct classification of each component in terms of ductility, using, for example, the three ductility classes proposed by Kuhlmann et al. [10]:

Class 1—components with high ductility ($\varphi_i \geqslant \alpha$).
Class 2—components with limited ductility ($\beta \leqslant \varphi_i < \alpha$).
Class 3—components with brittle failure ($\varphi_i < \beta$).

α and β representing ductility limits for the various component classes, here suggested as $\alpha = 20$ and $\beta = 3$. In design terms, and in-line with the usual assumptions in plastic design, it seems reasonable to assume, for Class 1 components, a ductility index $\varphi_i = \infty$. On the other end, for Class 3 components, because of brittle behaviour, a safe estimate can be obtained with a ductility index of $\varphi_i = 1$ (elastic response). For Class 2 components, lower bounds for the ductility indexes must be established for each component type, as a result of experimental and analytical research to be carried out. As a crude indication, from the experimental results obtained by Kuhlmann [9] and referring to Fig. 8, a ductility index in the range of 4–5 seems reasonable for the component web in compression, if a negative plastic stiffness is used.

7.2. Application to end-plate beam-to-column joints

Evaluation of the ductility indexes for test 109.005 yields the results of Table 7. Examination of Table 7

Table 7
Ductility indexes for extended end-plate joint 109.005

Component	$\varphi_i(\Delta_i^f/\Delta_i^y)$	Component "yield" sequence (j)									Failure
		Abs. displ. Δ_i				Rel. displ. Δ_i/Δ_i^y					
1	INF	−0.8899	−2.1079	−3.7941	−5.6194	−8.0380	1.0000	2.3687	4.2635	6.3146	9.0325	9.0325
2	5	0.2211	−0.2449	−1.0969	−2.0192	−3.2412	0.9028	1.0000	4.4790	8.2450	13.235	13.235
3.1	INF	0.2056	0.2276	0.2583	3.1832	7.0365	0.7960	0.8811	1.0000	12.324	27.242	27.242
3.2	INF	0.1581	0.1752	0.1987	0.2241	0.2583	0.6121	0.6783	0.7693	0.8676	1.0000	1.0000
4.1	INF	0.0820	0.0908	0.1030	0.1163	0.1338	0.7051	0.7807	0.8856	1.0000	1.1505	1.1505
4.2	INF	0.0631	0.0699	0.0792	0.0894	0.1030	0.5426	0.6010	0.6810	0.7687	0.8856	0.8856
5.1	INF	0.0128	0.0141	0.0160	0.0181	0.0208	0.4896	0.5393	0.6120	0.6923	0.7956	0.7956
5.2	INF	0.0096	0.0107	0.0121	0.0137	0.0157	0.3672	0.4093	0.4628	0.5240	0.6005	0.6005
10.1	1	0.2342	0.2593	0.2943	0.3321	0.3820	0.4838	0.5356	0.6079	0.6860	0.7891	0.7891
10.2	1	0.1801	0.1996	0.2263	0.2553	0.2943	0.3720	0.4123	0.4675	0.5274	0.6079	0.6079
Joint		0.0036	0.0086	0.0189	0.0326	0.0565	1.0000	2.3889	5.2500	9.0556	15.689	15.689
Rotation		Abs. rot. (radian)				Rel. rot. θ/θ_1						

clearly shows the "yield" sequence of the various components and the corresponding levels of ductility for the analysed extended end-plate joint. As also observed in Fig. 16, the first component to yield is the column web in shear, at a yield displacement of 0.8899 mm (Table 7) and a total joint rotation of 0.0036 radian, the other components remaining elastic. Next, in succession, the following components reach yield: column web in compression (2), column web in tension (3.1), column flange in bending (4.1) and column web in tension (3.2). Table 7 illustrates the relevant values of displacement and the corresponding values for the remaining components. Finally, for this test, the maximum recorded value of total rotation was 0.056 radian.

A joint ductility index can also be proposed, defined as

$$\varphi_j = \frac{\theta_f}{\theta_1} \tag{35}$$

where θ_f denotes the rotation at failure and θ_1 the rotation when the first component reaches its elastic limit. For the four examples presented above, the joint ductility index varies between 5 and 43, based on the maximum experimentally recorded rotation for each test. It is noted that except for test 109.003, no brittle components reached yield, casting some doubts over the likelihood of this particular result, since no sudden failure of the joint was subsequently observed. Also of importance is the maximum ductility index reached by the components with limited ductility, a maximum ratio of 46 being calculated for the column web in compression without failure.

8. Conclusions

The evaluation of the ductility of a steel joint within the scope of the component method requires proper characterisation of each component. A good balance between relative simplicity and rigorous results may be achieved using bi-linear approximations of the force–deformation behaviour of each component, including the post-limit stiffness. Because many components are still not adequately characterised, work remains to be done in that area before ductility indexes can be established for each component that, dependant on its geometric and material properties, correspond to safe estimates of deformation ability for each component.

This explains some less plausible results for the yield sequence of the various components that may arise from a certain conservative evaluation of the yield strength of some components. A good example of such a situation is the column web in compression, improved expressions

Table 8
Proposed code coefficients for the evaluation of rotation capacity

Component	Application rules			
	Resistance	Rotation capacity		
		Initial stiffness	Post-limit stiffness $\overline{K}_i$	Limit displacement
1 Column web panel in shear	$V_{wp,Rd} = \frac{0.9 f_{y,wc} A_{vc}}{\sqrt{3}\gamma_{M0}}$	$K_1 = E\frac{0.38 A_{vc}}{\beta z}$	[4.6%]	$\Delta_1^f = \infty$
2 Column web in compression	$F_{c,wc,Rd} = \frac{\omega b_{eff,c,wc} t_{wc} f_{y,wc}}{\gamma_{M0}}$ but $F_{c,wc,Rd} \leqslant \frac{\omega \rho b_{eff,c,wc} t_{wc} f_{y,wc}}{\gamma_{M1}}$	$K_2 = E\frac{0.7 b_{eff,c,wc} t_{wc}}{d_c}$	[2.3%]	$\Delta_2^f = [3-5]\Delta_2^y$
3 Column web in tension	$F_{t,wc,Rd} = \frac{\omega b_{eff,t,wc} t_{wc} f_{y,wc}}{\gamma_{M0}}$	$K_3 = E\frac{0.7 b_{eff,t,wc} t_{wc}}{d_c}$	[0.1–1.7%]	$\Delta_3^f = \infty$
4 Column flange in bending	Equivalent T-stub model [Annex J-EC3, J.3.2]	$K_4 = E\frac{0.85 l_{eff} t_{fc}^3}{m^3}$	[1.3%]	$\Delta_4^f = \infty$
5 End-plate in bending	Equivalent T-stub model [Annex J-EC3, J.3.2]	$K_5 = E\frac{0.85 l_{eff} t_p^3}{m^3}$	–[a]	$\Delta_5^f = \infty$
7 Beam or column flange and web in compression	$F_{c,fb,Rd} = \frac{M_{c,Rd}}{z}$	$K_7 = \infty$	–[a]	$\Delta_7^f = [3-5]\Delta_7^y$
8 Beam web in tension	$F_{t,wb,Rd} = \frac{b_{eff,t,wb} t_{wb} f_{y,wb}}{\gamma_{M0}}$	$K_8 = \infty$	–[a]	$\Delta_8^f = \infty$
10 Bolts in tension	$F_{t,Rd} = \frac{0.9 f_{ub} A_s}{\gamma_{Mb}}$	$K_{10} = E\frac{1.6 A_s}{L_b}$	Components with brittle failure	$\Delta_{10}^f = \Delta_{10}^y$
11 Bolts in shear	Varying according to bolt grade	$K_{11} = E\frac{16 n_b d^2 f_{ub}}{E d_{M16}}$	Components with brittle failure	$\Delta_{11}^f = \Delta_{11}^y$
19 Welds	$F_{w,Rd} = a\frac{f_u/\sqrt{3}}{\beta_w \gamma_{Mw}}$	$K_{19} = \infty$	Components with brittle failure	$\Delta_{19}^f = \Delta_{19}^y$

[a] Values to be established.

for its resistance being recently proposed by Kuhlmann and Kuenhemund [11].

The current draft version of Part 1.8 of EC3 [3] already tries to extend the vague ductility provisions that were present in Annex J of EC3 by presenting a table with an unfilled column for rotation capacity, component by component. Table 8 presents an improved version of this table which includes two columns for rotation capacity: post-limit stiffness and limit displacement. This subdivision is required since no ductility limits may be evaluated without the prior knowledge of a post-limit stiffness [13]. Based on the statistical analysis performed in this paper for a limited number of test results (single-sided, extended end-plate beam-to-column joints with backing plates between an IPE beam and a HEB column), some trial values are proposed (in brackets) as a first approximation.

Next, a ductility model is required which is able to predict the "yield" sequence of the various components [14] and a safe (lower bound) joint ductility index, here chosen as a relative value of total rotation with respect to the initial stiffness of the joint.

Finally, it is worth pointing out that ductility evaluation should be performed on actual values of component behaviour (particularly when talking in terms of strength), because of the unexpected results of over-strength effects that may produce unsafe results [15]. This may even lead to the requirement of guaranteed upper bounds on material properties, in particular for the yield stress of steel.

Acknowledgements

Financial support from Ministério da Ciência e Tecnologia—PRAXIS XXI research project PRAXIS/P/ECM/13153/1998 is acknowledged.

References

[1] Cruz PJS, Silva LS, Rodrigues DS, Simões R. Database for the semi-rigid behaviour of beam-to-column connections in seismic regions. J Construct Steel Res 1998;46(120):1–3.
[2] CEN. Eurocode 3, ENV-1993-1-1, Revised Annex J, Design of Steel Structures, CEN, European Committee for Standardization, Document CEN/TC 250/SC 3-N 419 E, Brussels, 1998.
[3] CEN. Eurocode 3, prEN-1993-1-8: 20xx, Part 1.8: Design of Joints, Eurocode 3: Design of Steel Structures, Draft 2 Rev., 6 December 2000, CEN, European Committee for Standardization, Brussels, 2000.

[4] Faella C, Piluso V, Rizzano G. Structural steel semirigid connections: theory, design and software. Boca Raton, FL: CRC Press; 2000.
[5] Gebbeken N, Wanzek T, Petersen C. Semi-rigid connections T-stub model. München, Germany: Institut für Mechanik und Statik, Universitat des Bundeswehr München; 1997.
[6] Huber G, Tschemmernegg F. Modelling of steel connections. J Construct Steel Res 1998;45(2):199–216.
[7] Janss J, Jaspart JP. Strength and behaviour of in plane weak axis joints and of 3-D joints. In: Bjorhovde R, Colson A, Zandonini R, editors. Connections in steel structures. Proceedings of the International Workshop on Joints. New York: Elsevier Applied Science; 1987.
[8] Jaspart JP. Etude de la semi-rigidité des noeuds poutre-colonne et son influence sur la resistance des ossatures en acier. PhD thesis, Department MSM, University of Liége, Belgium, 1991 [in French].
[9] Kuhlmann U. Influence of axial forces on the component: web under compression. Proceeding of COST-C1 Working Group Meeting, C1/WG2/99-01. Thessaloniki, May 1999.
[10] Kuhlmann U, Davison JB, Kattner M. Structural systems and rotation capacity. Proceeding of COST Conference on Control of the Semi-rigid Behaviour of Civil Engineering Structural Connections, Liège, Belgium, 1998. p. 167–76.
[11] Kuhlmann U, Kuhnemund F. Proposal of a new design resistance of the joint component column web in compression, Internal Report. Stuttgart, Germany: University of Stuttgart; January 2001.
[12] LUSAS. Lusas Finite Element System, Lusas–User Manual, Version 13.3. FEA—Finite Element Analysis Ltd., Kingston-upon-Thames, England, 2000.
[13] Silva LS, Coelho AG, Neto EL. Equivalent post-buckling models for the flexural behaviour of steel connections. Comput Struct 2000;77:615–24.
[14] Silva LS, Coelho AG. A ductility model for steel connections. J Construct Steel Res 2001;57:45–70.
[15] Silva LS, Gervásio H, Rebelo C, Coelho AG. Assessment of overstrength effects in steel and composite connections using Monte Carlo methods. In: Proceedings of IABSE International Conference on Safety, Risk and Reliability Trends in Engineering, Malta, 21–23 March 2001. p. 229–30.
[16] Shi YJ, Chan SL, Wong YL. Modelling for moment rotations characteristics for end-plate joints. J Struct Engng 1996;122(11):1300–6.
[17] Weynand K, Jaspart JP, Steenhuis M. The stiffness model of revised Annex J of Eurocode 3. In: Bjorhovde R, Colson A, Zandonini R, editors. Connections in steel structures III. Proceedings of the 3rd International Workshop on Connections in Steel Structures. Trento, Italy, 1995. p. 441–52.
[18] Yee YL, Melchers RE. Moment–rotation curves for bolted connections. J Struct Engng ASCE 1986;112(3): 615–35.
[19] Zoetemeijer P. A design method for the tension side of statically-loaded bolted beam-to-column joints. Heron 1974;20(1):1–59.